TWO- AND THREE-DIMENSIONAL EFFECTS IN THE SIMULATION OF WIDE PLATE TESTS

I. C. Howard*, Z. H. Li†, D. P. G. Lidbury#, A. M. Othman§, R. Patel¥, A. H Sherry# and J. Simpson¶

The paper describes a sequence of two- and three-dimensional simulations using Ductile Damage Mechanics of the crack growth in two wide-plate tests of the AEA test programme. The plane strain simulations predicted well only the initial crack growth, whilst plane stress computer runs represented the latter section of the resistance curves. A series of models of one of the tests allowed the exploration of the influence of out-of-plane effects and of ways of modelling in three-dimensions the substantial amount of in-plane crack growth observed in the tests. The final simulation reproduced well the detailed crack growth as represented by the experimental beach marks.

INTRODUCTION

A continuing programme of collaboration between AEA Technology and SIRIUS is involved with the attempt to demonstrate the effectiveness of Damage Mechanics to predict the performance of structures with enough reliability to ensure practical confidence. Several tests performed at AEA Technology have been the basis of this work. Of the predictions for material on the upper shelf, successful simulations of Spinning Cylinder Tests 1 2 and 3 have been reported elsewhere (1, 2). Here, we report on work extending that to two of the large wide plate tests (GNSR/9 and CRAD/G10) performed at AEA Technology as part of the programme to assess the levels of conservatism inherent in applying conventional small-scale specimen fracture data to structural components.

THE TESTS, CRAD/G10 AND GNSR/9

These tests (3, 4) were performed at ambient temperature, on the upper shelf of the renormalised A533B Class 1 pressure vessel steel from which the specimens were made. The two experiments were designed so that the expected crack growth would take place under conditions of well-contained yielding, the plastic zone being confined to a region close to the crack tip. Stress-strain data for the material was obtained from conventional tensile specimens, and the material's crack growth resistance was measured in two CT tests, producing the data reproduced in Figure 1.

* SIRIUS, the University of Sheffield.
† BAe Airbus Division, Bristol.
# AEA Technology, Risley.
§ United Arab Emirates University, UAE.
¥ Nuclear Electric Ltd., Berkeley.
¶ Jaguar Cars Ltd., Coventry.

Both large-scale test specimens were cut from 70 mm thick plate, each one containing a through-thickness edge crack. The CRAD/G10 specimen was tested (3) in pure bending whilst the GNSR/9 test (4) had the applied loading controlled to maintain the specimen in pure tension. The data obtained from these tests are also reproduced in Figure 1.

The value of J at initiation was approximately the same for the CRAD/G10 and GNSR/9 specimen tests, close to that found in the small scale CT specimens. The slope of the J-R curve for the CRAD/G10 specimen was very similar to that of the CT specimens up to about 2 mm of crack growth, after which the former was steeper. However, the slope for the pure tension GNSR/9 specimen was significantly greater. Details of the tests are summarised in Reference (5). In both tests, there was considerable crack tunnelling, with details of the process being revealed on the subsequent fracture surfaces by beach marks created by a series of unloadings. The appearance of the CRAD/G10 fracture surface is shown in Figure 2. The maximum amount of growth in both tests ocurred at the specimen centre, being about 32 mm for CRAD/G10 and 44 mm for GNSR/9. As Figure 2 shows, there was no flat crack growth at the specimen surfaces for CRAD/G10. However, some flat crack growth did occur at the surfaces of GNSR/9.

MATERIAL MODELLING

Damage in the material was described through the use of the Rousselier model (6), which uses a modified plastic potential of the form

$$F = \frac{\sigma_{eq}}{\rho} - H + \sqrt{3}DB(\beta)e^{\left(\frac{C\sigma_m}{\rho\sigma_Y}\right)} \qquad (1)$$

Here, H characterises the material work hardening, σ_{eq} is the equivalent stress and ρ is the material density. Together, the first two terms represent yielding by the usual J_2 theory. The third term represents the softening of the material due to damage and void growth. β is the damage variable and $B(\beta)$ is a function that also depends on C, the yield stress and f_0, the initial void volume fraction.

The parameters C and D are material constants which control the rate of damage evolution and are tuned for a particular material through a 'trial and error' series of numerical simulations of experimental data until the experimental results are replicated. There is also the size, L, of the damage cell, the most sensitive parameter in tuning. Numerical experimentation eventually produced the model that had the simulated CT resistance curve shown in Figure 1. This was obtained with the parameters of L = 0.25 mm, C = 0.98 and D = 2.0. The initial void volume fraction was estimated to be $f_0 = 9.33\times10^{-4}$ in the usual way (5).

SIMULATION OF THE TESTS

The behaviour of the two tests was simulated by a series of two- and three-dimensional models. Some results of the 2-D simulations have been reported elsewhere (5); the predicted J-resistance curves are shown in Figure 1, together with the experimental data of the two large-scale tests and the CTS data.

Two-Dimensional Modelling

The two-dimensional meshes used to analyse both tests were very similar. In particular, the mesh configuration ahead of the crack tip was identical to that used for the CTS analyses that formed the basis of our tuning of the damage mechanics parameters of this material.

The initial 2-D crack growth predictions of both tests compare well with that measured experimentally, but the plane strain simulations significantly underestimate the observed crack growth resistance after that. However, the runs in plane stress do represent reasonably well the latter sections of the resistance curves. This 2-D work strongly suggested that both wide-plate tests began their crack growth under plane strain constraint, but, after about 3 or 4 mm of growth, the constraint on the crack tip material changed to that of plane stress. If so, the crack growth in both tests would be strongly influenced by three-dimensional effects. Further evidence for that comes from the fully 3-D nature of the flat crack growth as exemplified by the curved beach marks and final crack border seen on the fracture surface of CRAD/G10, and shown in Figure 2.

The resolution of this requires three-dimensional simulation.

Three-Dimensional Modelling

Both of the tests were simulated with three-dimensional Ductile Damage Mechanics models. Since the GNSR 9 test involved considerably greater crack growth than CRAD/G10, the size of the model was also greater, as is necessary for models that have the same cell size in the region near the tip into which the crack is expected to grow. As a result, the execution time for the GNSR/9 simulation was very much greater than that of the other test. The amount of growth achieved in the 300 hours of CPU time devoted to the GNSR/9 simulation was much smaller than that revealed by the first beach mark. This happened at a load of about 25% of the measured value. Even so, the displacement was no more than about 5% of the measured value, demonstrating that the realistic simulation of this particular test was beyond the computing power available at the time.

The computed distributions of the value of J along the crack border in both tests were approximately uniform at the lowest applied loads, and then, as loads increased, began to show a distinct "bowing" towards the centre. This reflects the variation of crack driving force that corresponds with the evolving shape of the crack fronts. For the relatively low values of load achievable in the GNSR/9 simulation, however, there did appear to be a greater tendency for J to increase at the surfaces than that exhibited in the CRAD/G10 simulation. This is a very satisfactory correspondence with the observed surface growth in the GNSR/9 test.

As a result, the assessment of crack growth was concentrated on the analysis of test CRAD/G10. The modelling of this is shown in Figure 3, and Figure 4 illustrates the finite element mesh employed. The method used for advancing the simulated crack assumes (1) the crack tip moves forward one cell unit on the attainment of the load peak in the appropriate cell immediately ahead of the current crack tip. Figure 5 compares the simulated and experimental positions of the crack front at a clip-gauge reading corresponding to Beach Mark 3. This was the largest amount of simulated growth achieved in the computations, because, at higher loads, the calculations tended to become unstable.

The results illustrated in Figure 5 are very satisfactory. They show that, with care, it is possible to model complex crack growth accurately using the techniques of Ductile

Damage Mechanics, both in terms of the amount of growth and the shape of the crack front.

DISCUSSION

Whilst the agreement between experiment and simulation discussed above is very encouraging, there are several issues arising from these studies that require consideration and, perhaps, further research. The first is the balance between acceptable computing times and simulation accuracy in three dimensional work. The results reported above are from the most recent (7) work. In this, the aspect ratio of the Damage Mechanics cell through which the simulate crack is to grow is seven. Previous 3-D work (8) had shown that there is a small mesh refinement effect on the shape of the predicted growing crack in studies that examined variations simulated with aspect ratios of 28 and 14. Detailed examination of this evidence was enough to suggest that the 7:1 ratio used to produce the results of Figure 5 was reasonable, both in terms of predicted crack shape and the amount of growth, but this conclusion is not absolute.

A feature of the tests that has not been simulated is the shearing observed near the surfaces in both tests. Whether Ductile Damage Mechanics models of the type used here can deal with these was not explored in this work. This could fruitfully form the basis of further work.

REFERENCES

(1) Bilby, B.A., Howard, I.C. and Li, Z.H. (1993), Prediction of the First Spinning Cylinder Test using Ductile Damage Theory. Fatigue and Fracture of Engineering Materials and Structures, **16**, 1- 20.

(2) Bilby, B.A. *et al.*, (1994), Prediction of Spinning Cylinder Tests 2 and 3 Using Continuum Damage Mechanics. in H. Mehta (ed.), *Fracture Mechanics Applications*, PVP Vol.287/MD-Vol. 47, American Society of Mechanical Engineers, New York, pp 3-10.

(3) Sharples, J.K. et al. (1993), Report of CRAD/G10 large-scale test carried out on renormalised A533B -1 steel plate containing through-thickness crack loaded under in-plate bending, AEA Technology Reactor Services, Risley.

(4) Sharples, J.K. *et al.*, (1993), Report of first ductile tearing test performed on wide-plate GNSR/9. AEA Technology Reactor Services, Risley.

(5) Howard, I. C., Othman, A. M., Lidbury, D. P. G., and Sherry A. H., (1996), Simulation of the behaviour of two large scale tests using ductile damage mechanics models derived from small scale laboratory data, in Proc. IUTAM Symposium on "Micromechanics of Plasticity and Damage of Multiphase Materials", Sevres, France, 29 August -1 September 1995, Eds. A. Pineau and A. Zaoui, Kluwer Academic Publishers, 199 -206.

(6) Rousselier, G. (1987), Ductile Fracture Models and their Potential in Local Approach of Fracture. *Nuclear Engineering and Design*, **105**: 97-111.

(7) Simpson, J. T. (1997), Three dimensional simulation of AEA wide-plate tests CRAD/G10 and GNSR/9, Project Report, Department of Mechanical Engineering, the University of Sheffield.

(8) Patel, R. D. (1996), Three dimensional simulation of AEA wide-plate tests CRAD/G10 and GNSR/9, Project Report, Department of Mechanical Engineering, the University of Sheffield.

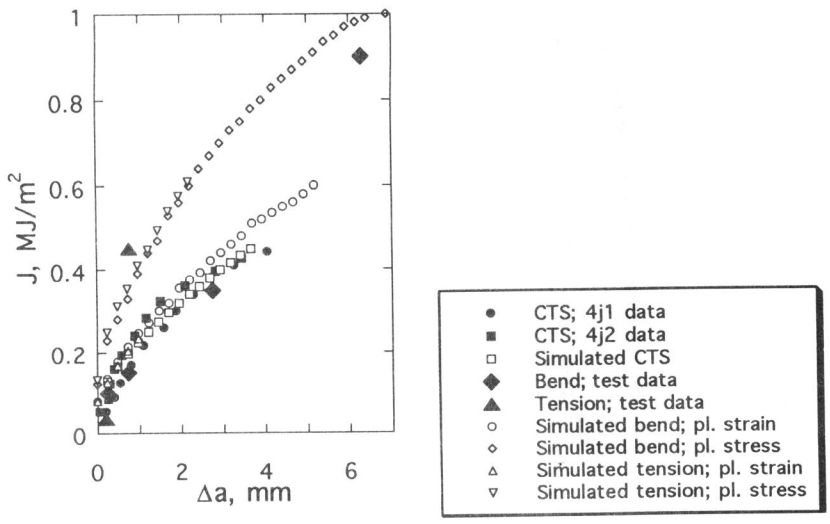

Figure 1. Experimental and simulated J-resistance curves of CT specimens and the two wide plate tests.

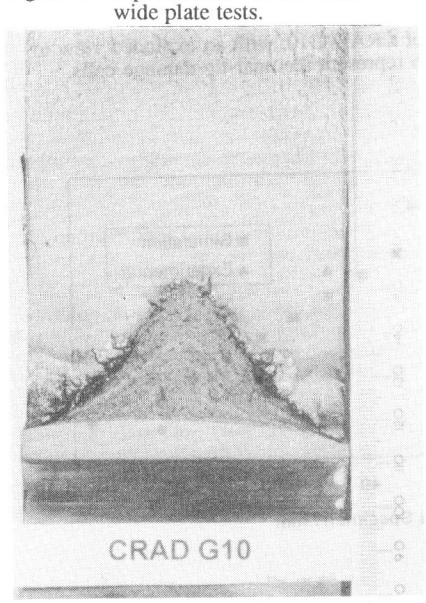

Figure 2. Details of the fracture surface of CRAD/G10.

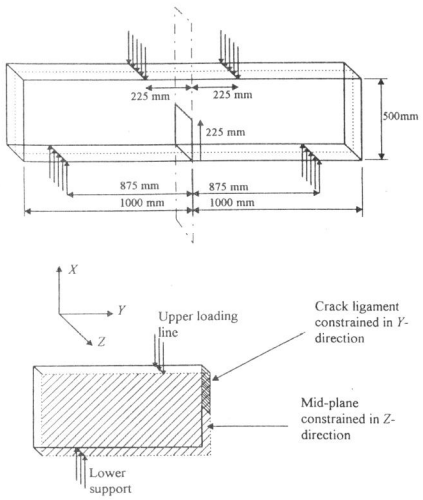

Figure 3. The modelling of CRAD/G10.

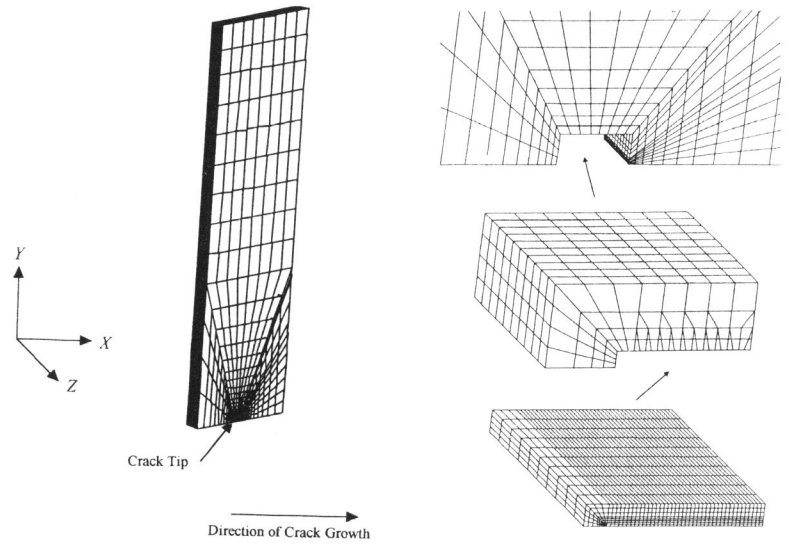

Figure 4. The mesh used in the modelling of CRAD/G10, with an exploded view to show the refinement required to represent the near-tip damage cells.

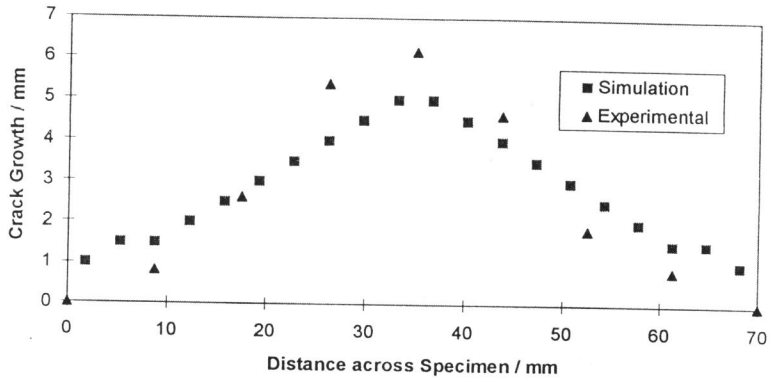

Figure 5. The simulated and measure crack growth at a clip-gauge value corresponding with Beach Mark 2.